Hyperspectral Image Classification Based on Nonlinear Spectral-Spatial Network

Bin Pan, Zhenwei Shi, Ning Zhang and Shaobiao Xie

Abstract

Recently, for the task of hyperspectral images classification, deep learning-based methods have revealed promising performance. However, the complex network structure and time-consuming training process have restricted their applications. In this letter, we construct a much simpler network, nonlinear spectral-spatial network (NSSNet), for hyperspectral images classification. NSSNet is developed from the basic structure of PCA network. Nonlinear information is included in NSSNet, so as to generate more discriminative feature expression. Moreover, spectral and spatial features are combined to further improve the classification accuracy. Experimental results indicate that our method achieves better performance than state-of-the-art deep learning-based methods.

Index Terms

Hyperspectral image classification, deep learning, NSSNet.

I. INTRODUCTION

Hyperspectral remote sensing is an advanced earth observation tool, which is developed based on spectroscopy technique. Hyperspectral imaging sensors can provide data with spatial and spectral information simultaneously. Hundreds of contiguous and narrow spectral bands values are recorded as a data cube, with the spectral resolution up to nm-level. A common application of the hyperspectral data is materials classification for each pixel. In the last decade, plenty of hyperspectral image classification methods have been developed. Researchers usually design reliable classifiers [1], [2], [3], or further utilize spatial-spectral information [4], [5], [6], [7].

Bin Pan is with Image Processing Center, School of Astronautics, Beihang University, Beijing 100191, China, and with Beijing Key Laboratory of Digital Media, Beihang University, Beijing 100191, China, and also with State Key Laboratory of Virtual Reality Technology and Systems, School of Astronautics, Beihang University, Beijing 100191, China, (e-mail: panbin@buaa.edu.cn).

Zhenwei Shi (Corresponding Author) is with Image Processing Center, School of Astronautics, Beihang University, Beijing 100191, China, and with Beijing Key Laboratory of Digital Media, Beihang University, Beijing 100191, China, and also with State Key Laboratory of Virtual Reality Technology and Systems, School of Astronautics, Beihang University, Beijing 100191, China, (e-mail: shizhenwei@buaa.edu.cn).

Ning Zhang is with Shanghai Aerospace Electronic Technology Institute, Shanghai, 201109, China, (e-mail: dzs_zhangning@163.com).

Shaobiao Xie is with Shanghai Academy of Spaceflight Technology, Shanghai, 201109, China, (e-mail: boyish9747@outlook.com).

Recently, deep learning-based algorithms have been introduced to hyperspectral image classification, and presented promising performance. The idea of deep learning is to extract higher level features which represents more abstract semantics of the original data. To put it simply, deep learning may be considered as a nonlinear feature expression process, while the network structure could be regarded as the mapping relationship. Autoencoder (AE) is a popular deep architecture-based models. In [8], Chen *et al.* proposed a deep learning framework to deal with hyperspectral image classification for the first time, where AE is used to learn deep features of hyperspectral data in an unsupervised manner. Then in [9], the framework was improved by Deep Belief Network (DBN). Some variations of AE were studied in literatures, such as stacked denoising autoencoders [10], [11] and convolutional autoencoder [12]. Another kind of deep learning method, convolutional neural networks (CNN), were also reported in recent research on hyperspectral image classification [13], [14], [15]. However, deep learning methods usually suffer from complex network structure and time-consuming training process. Many tricks have to be used in the process of designing the basic structure of the network, and the experimental results are difficult to reproduce.

In this letter, we propose a nonlinear spectral-spatial network (NSSNet) for hyperspectral image classification, which is developed from PCA network (PCANet) [16]. PCANet is a much simpler network while it is already on par with state-of-the-art deep learning-based methods for many image classification tasks [16]. Motivated by this, we attempt to propose a new network for hyperspectral image classification whereas achieve better performance than deep learning methods. However, the spectral data cannot be directly utilized by PCANet. Moreover, spatial information, which provides additional discriminant information that may lead to more accurate classification results, is not considered by PCANet. In this letter, we propose a novel joint spectral-spatial network utilizing the spectral and spatial information simultaneous. Furthermore, considering that nonlinear information may generate more discriminative feature expression for each pixel, we improve the structure of PCANet by adding some nonlinear elements. Our work can be regarded as a simplified deep learning method, but better performances are observed in the experiments.

The remainder of this letter is organized as follows. In section II we present detailed description of the proposed NSSNet-based hyperspectral image classification method. Section III reports the experimental comparison with state-of-the-art deep learning-based methods. Conclusions are drawn in Section IV.

II. NSSNet-based Hyperspectral Image Classification

The NSSNet-based hyperspectral image classification method includes two parallel modules: spectral and spatial features extraction. In each module, different imaging strategy is adopted to generate 2-D samples, and an improved PCANet with nonlinear information is followed for feature extraction. Then, we fuse the spectral and spatial features, and SVM is used to obtain the final results. The flowchart of our NSSNet-based method is shown in Figure 1. In this section, we first give a brief introduction to PCANet, and then, we discuss how nonlinear information is used to improve the performance of our network. Finally, spectral and spatial information are combined to construct the proposed NSSNet.
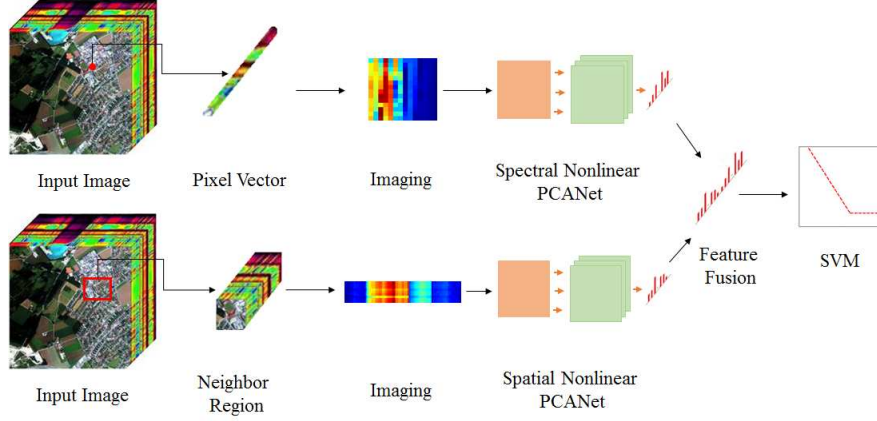
Fig. 1. Flowchart of the NSSNet method.

A. A Brief Introduction to PCANet

PCANet is first proposed to handle the task of classification for single image. The works about PCANet try to achieve two goals: First, designing a simple deep learning network. Second, providing a baseline for different tasks where more advanced and sophisticated architectures can be utilized [16]. Compared with CNN, the most important change in PCANet is that the original data-adopting convolution filter banks between layers are replaced by basic PCA filters, and thus the complex supervised optimizing process is avoided. Furthermore, binary quantization (hashing), histogram features and linear support vector machine (SVM) are also adopted to simplify traditional deep learning methods such as CNN. Generally, PCANet contains three processing components: PCA filters, binary hashing, and histogram features. More details are shown in [16].

PCA filters are used to construct a cascaded network. Suppose $\mathbf{I}_i$ is a given input image of size $m \times m$. PCANet first take a $k_1 \times k_2$ patch around each pixel, and collect all the vectorized patches, the mean values of which have been removed, to form a matrix $\mathbf{X_i} \in \mathbb{R}^{(k_1 k_2) \times n}$, where n is the number of patches extracted from $\mathbf{I}_i$. Then, construct the same matrix for each input image and combine all the matrices:

$$\mathbf{X} = [\mathbf{X_1}, \mathbf{X_2}, \ldots, \mathbf{X_N}] \in \mathbb{R}^{(k_1 k_2) \times (Nn)}, \tag{1}$$

where N is the number of input images. PCA minimizes the reconstruction error within a family of orthonormal filters:

$$\min_{V \in \mathbb{R}^{(k_1 k_2) \times L_1}} \|\mathbf{X} - \mathbf{V}\mathbf{V^T}\mathbf{X}\|_F^2, \text{s.t.} \mathbf{V^T}\mathbf{V} = \mathbf{E}_{L_1}, \tag{2}$$

where $\mathbf{E}$ is an identity matrix with size $L_1 \times L_1$, $\mathbf{V}$ are the principal eigenvectors of $\mathbf{X}\mathbf{X^T}$, and L_1 denotes the number of principal eigenvectors. In PCANet, L_1 also corresponds to the number of filters in the first layer. Therefore, the filters can be expressed as

$$\mathbf{W}_l^1 \doteq \text{mat}_{(k_1 k_2)}(q_l(\mathbf{X}\mathbf{X^T})) \in \mathbb{R}^{k_1 \times k_2}, l = 1, 2, \ldots, L_1, \tag{3}$$

where $\mathrm{mat}_{(k_1 k_2)}(\cdot)$ is a function that reshapes a vector to a matrix, and $q_l(\mathbf{XX^T})$ denotes the l-th principal eigenvector of $\mathbf{XX^T}$. Then, the first layer of PCANet can be obtained by

$$\mathbf{I}_i^l \doteq \mathbf{I}_i * \mathbf{W}_l^1, i = 1, 2, \ldots, N. \tag{4}$$

Conducting the same process as in the first layer for all the obtained $\mathbf{I}_i^l$, the second layer of PCANet is obtained. Assuming that the number of filters used in the second layer is L_2, PCANet would output $L_1 L_2$ images. One can build a multiple-layer PCA network, by repeating the above process, to extract higher level features. In [16], the authors suggested that two layers are enough for most tasks.

After establishing the structure of the network, a binary quantization process is followed. Subsequently, each of the L_1 images is separated into many local blocks. The histogram of each block (with 2^{L_2} bins) is computed, and all the histograms are concatenated into one vector. This vector is the feature expression for image $\mathbf{I}_i$. Finally, a linear SVM is used to determine the classification results.

B. Nonlinear Information

Original PCANet is completely a linear network, where the construction of convolution kernels are simple PCA filters. By contrast, in typical (convolutional) deep learning-based methods such as CNN, the convolution kernels are obtained by complex nonlinear optimization process. In NSSNet, we adopt two nonlinear strategies, kernel method and nonlinear mapping, to improve the performance of PCANet. Note that although nonlinear information is added, the NSSNet is still much simpler than traditional deep learning-based methods.

Kernel method is an effective approach for transforming input data to a higher dimensional space. If the selected kernel meets the Mercer theorem, then the obtained space is actually a Reproducing Kernel Hilbert Space. In NSSNet, we utilize the Kernel PCA (KPCA) to replace the original PCA filter in PCANet. KPCA is a nonlinear extension of classical PCA. Compared with PCA, KPCA is able to capture the nonlinear information among input data, while requires nothing about the data distribution in the original space. Based on KPCA, we modify the construction of filters by:

$$\mathbf{KW}_l^j \doteq \mathrm{mat}_{(k_1 k_2)}(\psi_l(K(\mathbf{x}_a, \mathbf{x}_b))) \in \mathbb{R}^{k_1 \times k_2}, l = 1, 2, \ldots, L_j, \tag{5}$$

where $K(\mathbf{x}_a, \mathbf{x}_b)$ is a kernel function, $\mathbf{x}_a, \mathbf{x}_b \in \mathbf{X}$ are column vectors, j is the j-th layer, and $\psi_l(\cdot)$ denotes the l-th principal dimension-reduced data. Instead of using principal eigenvectors, in NSSNet we construct the filter banks by the dimension-reduced data directly, because KPCA cannot give the explicit eigenvectors for the input data. Eq. (5) indicates that the inner product operation is simply replaced by a kernel function. Consequently, the computation cost does not increased a lot. There are many popular kernel functions can be used, such as linear kernel, Radial Basis Function (RBF) kernel and polynomial kernel. In NSSNet, the most popular kernel, RBF, is adopted, which is defined by

$$K(\mathbf{x}_a, \mathbf{x}_b) = \exp(-\frac{\|\mathbf{x}_a - \mathbf{x}_b\|^2}{2\sigma^2}), \tag{6}$$

where σ is a parameter that controls the width of radial basis function.

To further enhancing the nonlinear structure, we introduce nonlinear mapping for the NSSNet. In traditional deep learning-based methods such as CNN, the hidden neurons usually include a *Sigmoid* function for nonlinear mapping. This strategy can not only avoid the multilayer networks equalling to single layer, but also extract more nonlinear information from the original data. However, in PCANet, there is no nonlinear mapping between layers. In NSSNet, we improve the original PCANet by adding *Sigmoid* function to the convolved results, which can be mathematically expressed by

$$\mathbf{I}_{nl}^i = \frac{1}{1 + \exp(-\mathbf{I}_l^i)} \tag{7}$$

Note that the nonlinear mapping is conducted on $\mathbf{I}_l^i$.

Overall, both kernel method and *Sigmoid* function are used in NSSNet, so as to extract nonlinear information in hyperspectral data.

C. Spectral-Spatial Classification Network

The inputs for PCANet are many single images, and the goal of PCANet is determining the label of each image. However, in hyperspectral image classification, we aim at giving a label to each pixel which is represented by a observed 1-D spectrum. Furthermore, it has been proved by many researchers that spatial information can significantly improve the classification accuracy, while the original PCANet does not consider the spatial relationship. In NSSNet, we propose the imaging strategy to handle the problem of hyperspectral image classification. Spectral and spatial features are extracted by different imaging methods, and a feature fusion process is followed to obtain the final feature expression for each pixel.

1) Spectral Feature Extraction: Instead of using the spectra vectors directly, we first conduct data imaging. Data imaging refers to transform a 1-D vector to a 2-D image. Let $\mathbf{y}_i \in \mathbb{R}^p$ denote an observed spectrum vector of a pixel, then the imaging form of $\mathbf{y}$ can be expressed by

$$\mathbf{y}_i \xrightarrow{\text{reshape}} \mathbf{Y}_i^{Spec} \in \mathbb{R}^{k \times k}. \tag{8}$$

Here we set the width and height of the imaged data the same for simplifying. In the imaging process, the reflectance value in each band of a pixel vector is considered as the "texture" in an image. Compared with real-world images, the generated imaging data can be regarded as texture-stable images which are immune to illumination, scales and rotation. By this means the problem of hyperspectral image classification is transformed to image classification. Subsequently, the improved nonlinear-PCANet is used to extract the feature extraction for each pixel. Some samples of imaged spectra for *Indian Pines* dataset are shown in Figure 2(a).

2) Spatial Feature Extraction: Researchers have verified that spatial information can significantly improve accuracy of deep learning-based hyperspectral image classification [8], [9]. In NSSNet, we construct an image for each pixel by utilizing the spectra of the pixel and its neighbors. Different from the imaging process for spectral information, for a pixel spectrum $\mathbf{y}_i$, here we connect $\mathbf{y}_i$ and its neighbors side by side, which can be denoted by

$$[\mathbf{y}_{i-s}, \ldots, \mathbf{y}_i, \ldots, \mathbf{y}_{i+s}] \xrightarrow{\text{reshape}} \mathbf{Y}_i^{Spat} \in \mathbb{R}^{s^2 \times p}, \tag{9}$$

(a)

(b)
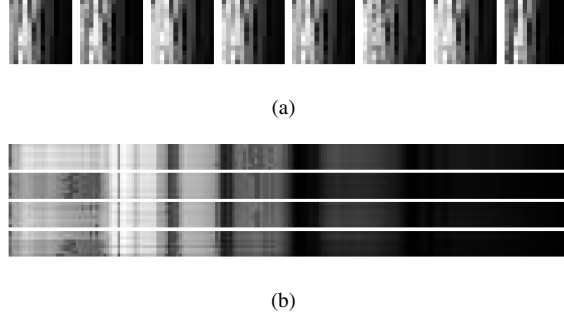
Fig. 2. Samples of imaged data. (a) Spectral images. (b) Spatial images.

where $s \times s$ is the window size for a pixel. Generally, 3×3 is appropriate to describe the spatial information. We adopt this imaging strategy mainly because the spatial correlation between pixel and its neighbors is an important concern. Some samples of spatial imaged data for *Indian Pines* dataset are displayed in Figure 2(b). Note that this is only an available imaging method, other similar approaches also work.

After extracting the spectral and spatial features, we directly connect them to compose the final feature expression for each pixel. At last, a SVM classifier is used to determine the labels, which is also adopted in original PCANet [16].

III. EXPERIMENTAL RESULTS

A. Datasets and Experimental Setup

Two popular real-world hyperspectral images are used in the experiments, namely *Indian Pines* and *Pavia University* scenes[1].

- Indian Pines image was collected by airborne visible/infrared imaging spectrometer (AVIRIS) in Northwestern Indiana, with 145×145 pixels size. After removing the water-absorption bands, 200 spectral bands remain in this image. There are totally 10249 labeled pixels in the ground truth, and they are classified into 16 classes (Figure 3(a-b)).

- Pavia University image was acquired by reflective optics system imaging spectrometer (ROSIS-3) sensor over the city of Pavia, Italy. The size of this image is 610×340, and 103 bands are used for classification after removing the noise bands. Totally 42776 labeled pixels are available in the ground truth, and contains 9 different classes (Figure 4(a-b)).

The labeled samples are randomly divided into training set and test set with a ratio of 1:1, as is adopted in [9], for a fair comparison. In addition, the default network parameters setting of PCANet is adopted by NSSNet: 2 layers, 7×7 patch size, 8 filters in each layer, 7×7 size of block histograms and 0.8 overlap ratio. As discussed in [16], different parameters only have slightly influence on the final results. Our unreported works also indicate the

---

[1]Available online: http://www.ehu.eus/ccwintco/index.php?title=Hyperspectral _Remote_Sensing_Scenes
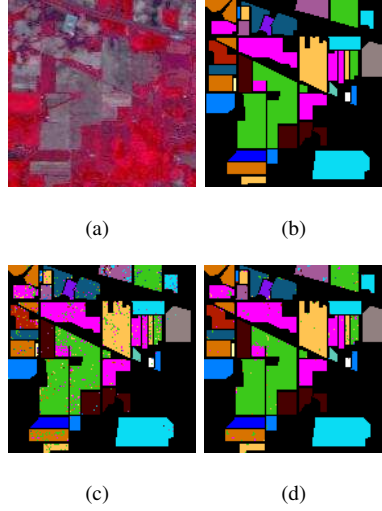
Fig. 3. Classification results for Indian Pines dataset. (a) False color composition image. (b) The ground truth. (c) Results of PCANet. (d) Results of NSSNet.
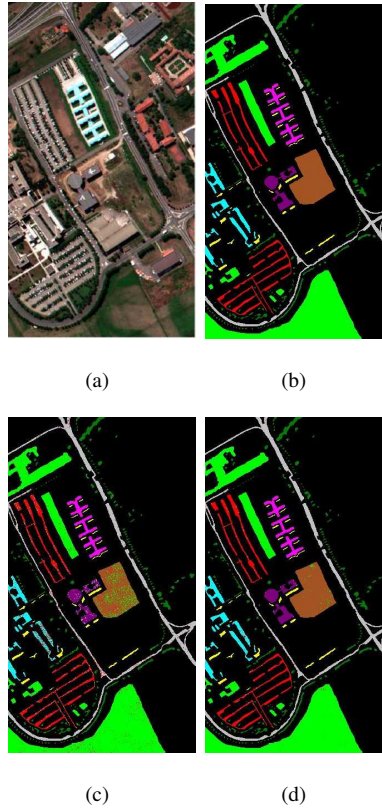
Fig. 4. Classification results for Pavia University dataset. (a) False color composition image. (b) The ground truth. (c) Results of PCANet. (d) Results of NSSNet.

same phenomenon. Therefore, the same setup as PCANet is used to construct the basic structure of NSSNet. Note that our spectral-based and spatial-based networks share the same parameters.

B. Compared Methods

Since we aim at designing a simple deep learning method for hyperspectral image classification, we compare our NSSNet with two state-of-the-art deep learning-based methods, SAE-LR [8] and DBN-LR [9]. Both spectral and spatial information are used in SAE-LR and DBN-LR. Furthermore, to demonstrate the effectiveness of the nonlinear and spectral-spatial joint information used in NSSNet, we also compare our method with original PCANet [16]. However, as discussed above, original PCANet is used for single image classification, whereas it cannot be directly used for hyperspectral image classification. Here we adopt the same imaging process as NSSNet so that PCANet is able to conduct. In addition, a traditional method, Representative Multiple Kernel Learning (RMKL) [3], is also compared in the experiments.

TABLE I

CLASSIFICATION RESULTS AND TRAINING TIME FOR THE TWO DATASETS.

	Indian Pines				Pavia University			
	OA(%)	AA(%)	κ	Time(m)	OA(%)	AA(%)	κ	Time(m)
PCANet	86.58	85.16	0.8471	**12.4**	93.20	91.01	0.8997	**28.6**
RMKL	95.61	94.20	0.9499	-	96.06	94.48	0.9443	-
SAE-LR	92.58	90.38	0.9152	359.6	98.69	98.17	0.9829	1788.4
DBN-LR	95.95	95.45	0.9539	-	99.05	98.48	0.9875	-
NSSNet	**96.08**	**96.40**	**0.9547**	20.3	**99.50**	**99.03**	**0.9910**	66.1

C. Results and Discussion

The classification results for the two datasets by the original PCANet and the proposed NSSNet are depicted in Figure 3(c)-(d) and Figure 4(c)-(d). We can see that the performance of NSSNet is better than that of the PCANet, which may indicate that the nonlinear and spectral-spatial joint information have improved the feature expression capability of the network. In Table I, the quantified evaluation results about accuracies and running time are displayed. We note that all the compared methods perform well in hyperspectral image classification, while our method achieves the best results in both of the datasets. The NSSNet takes more time than PCANet in the training process, but the overall accuracies (OA) of the NSSNet surpass that of the PCANet by about 9.5 percentages in Indian Pines image and 6.2 percentages in Pavia University image, which verifies the effectiveness of our improvements. Similar results are also observed in average accuracies (AA) and Kappa coefficients (κ). The accuracies of RMKL are lower than that of the proposed method, especially in Pavia University dataset. The reason may be that Pavia University dataset can provide more training sample, which would improve the performance of the proposed method significantly. Compared with SAE-LR and DBN-LR, the NSSNet outperforms them slightly. However, as discussed in [8] and [9], the training process of deep learning-based methods is quite time-consuming, and usually requires special as well as expensive equipments (such as GPUs). For example, the training time of

SAE-LR for Pavia University image is up to 1788.4 minutes[2], while the same process of NSSNet takes only 66.1 minutes. The NSSNet performs similarly, and even better, when compared with some state-of-the-art deep learning-based methods, whereas it has simpler network structure and faster processing speed.

Furthermore, we also perform a paired t-test between NSSNet and DBN-LR methods to validate whether the observed improvements in OA is statistically significant (at confidence level 95%) [9]. We assume that the mean OA of NSSNet ($\overline{a_1}$) is larger than that of DBN-LR ($\overline{a_2}$). We accept the hypothesis only if

$$\frac{(\overline{a_1} - \overline{a_2})\sqrt{n_1 + n_2 - 2}}{\sqrt{(\frac{1}{n_1} + \frac{1}{n_2})(n_1 s_1^2 + n_2 s_2^2)}} > t_{1-\alpha}[n_1 + n_2 - 2], \tag{10}$$

where s_1 and s_2 are the standard deviations of the two results, and n_1 and n_2 are the number of realizations of experiments reported which is set as 20 in this letter. For Indian Pines and Pavia University datasets, the standard deviations of our method are 0.1675% and 0.0853%, respectively. Therefore, the increases on OA are statistically significant (at the level of 95%) for the two test datasets.

Overall, we may infer from the experiments that the NSSNet is a promising and efficient method for the task of hyperspectral image classification.

IV. CONCLUSION

In this letter, we introduced a novel hyperspectral image classification framework, nonlinear spectral-spatial network. The NSSNet could be regarded as a simplified deep learning-based method, where the original hyperspectral data were transformed to a new feature space by nonlinear mapping. Furthermore, besides spectral features, the spatial information was also involved in the NSSNet, which has significantly improved the final classification results. Experiments indicated that the NSSNet outperforms some state-of-the-art deep learning-based methods. Future work will be devote to reducing the number of training samples and further improving the accuracies.

V. ACKNOWLEGEMENT

REFERENCES

[1] J. A. Gualtieri and R. F. Cromp, "Support vector machines for hyperspectral remote sensing classification," in *The 27th AIPR Workshop: Advances in Computer-Assisted Recognition*.   International Society for Optics and Photonics, 1999, pp. 221–232.

[2] M. Chi, Q. Kun, J. A. Benediktsson, and R. Feng, "Ensemble classification algorithm for hyperspectral remote sensing data," *Geoscience and Remote Sensing Letters, IEEE*, vol. 6, no. 4, pp. 762–766, 2009.

[3] Y. Gu, C. Wang, D. You, Y. Zhang, S. Wang, and Y. Zhang, "Representative multiple kernel learning for classification in hyperspectral imagery," *Geoscience and Remote Sensing, IEEE Transactions on*, vol. 50, no. 7, pp. 2852–2865, 2012.

[4] G. Camps-Valls, L. Gomez-Chova, J. Muñoz-Marí, J. Vila-Francés, and J. Calpe-Maravilla, "Composite kernels for hyperspectral image classification," *Geoscience and Remote Sensing Letters, IEEE*, vol. 3, no. 1, pp. 93–97, 2006.

---

[2]TITAN X, i7-6700K, 32G RAM, Theano

[5] L. Zhang, L. Zhang, D. Tao, and X. Huang, "On combining multiple features for hyperspectral remote sensing image classification," *Geoscience and Remote Sensing, IEEE Transactions on*, vol. 50, no. 3, pp. 879–893, 2012.

[6] X. Kang, S. Li, and J. A. Benediktsson, "Spectral–spatial hyperspectral image classification with edge-preserving filtering," *Geoscience and Remote Sensing, IEEE Transactions on*, vol. 52, no. 5, pp. 2666–2677, 2014.

[7] J. Li, X. Huang, P. Gamba, J. M. Bioucas-Dias, L. Zhang, J. Atli Benediktsson, and A. Plaza, "Multiple feature learning for hyperspectral image classification," *Geoscience and Remote Sensing, IEEE Transactions on*, vol. 53, no. 3, pp. 1592–1606, 2015.

[8] Y. Chen, Z. Lin, X. Zhao, G. Wang, and Y. Gu, "Deep learning-based classification of hyperspectral data," *Selected Topics in Applied Earth Observations and Remote Sensing, IEEE Journal of*, vol. 7, no. 6, pp. 2094–2107, 2014.

[9] Y. Chen, X. Zhao, and X. Jia, "Spectral–spatial classification of hyperspectral data based on deep belief network," *Selected Topics in Applied Earth Observations and Remote Sensing, IEEE Journal of*, vol. 8, no. 6, pp. 2381–2392, 2015.

[10] X. Ma, J. Geng, and H. Wang, "Hyperspectral image classification via contextual deep learning," *EURASIP Journal on Image and Video Processing*, vol. 2015, no. 1, pp. 1–12, 2015.

[11] Y. Liu, G. Cao, Q. Sun, and M. Siegel, "Hyperspectral classification via deep networks and superpixel segmentation," *International Journal of Remote Sensing*, vol. 36, no. 13, pp. 3459–3482, 2015.

[12] W. Zhao, Z. Guo, J. Yue, X. Zhang, and L. Luo, "On combining multiscale deep learning features for the classification of hyperspectral remote sensing imagery," *International Journal of Remote Sensing*, vol. 36, no. 13, pp. 3368–3379, 2015.

[13] K. Makantasis, K. Karantzalos, A. Doulamis, and N. Doulamis, "Deep supervised learning for hyperspectral data classification through convolutional neural networks," in *Geoscience and Remote Sensing Symposium (IGARSS), 2015 IEEE International*. IEEE, 2015, pp. 4959–4962.

[14] W. Hu, Y. Huang, L. Wei, F. Zhang, and H. Li, "Deep convolutional neural networks for hyperspectral image classification," *Journal of Sensors*, vol. 2015, 2015.

[15] H. Liang and Q. Li, "Hyperspectral imagery classification using sparse representations of convolutional neural network features," *Remote Sensing*, vol. 8, no. 2, p. 99, 2016.

[16] T.-H. Chan, K. Jia, S. Gao, J. Lu, Z. Zeng, and Y. Ma, "PCANet: A simple deep learning baseline for image classification?" *Image Processing, IEEE Transactions on*, vol. 24, no. 12, pp. 5017–5032, 2015.